

# Radiative Muon Capture by a Proton in Chiral Perturbation Theory

T. Meissner,<sup>1</sup>

*Department of Physics, Carnegie Mellon University,  
Pittsburgh, PA 15213, U.S.A.*

F. Myhrer<sup>2</sup> and K. Kubodera<sup>3</sup>

*Department of Physics and Astronomy,  
University of South Carolina, Columbia, SC 29208, U.S.A.*

---

## Abstract

The first measurement of the radiative muon capture (RMC) rate on a proton was recently carried out at TRIUMF. The TRIUMF group analyzed the RMC rate,  $\Gamma_{\text{RMC}}^{\text{exp}}$ , in terms of the theoretical formula of Beder and Fearing, and found the surprising result that  $g_P \equiv f_P(q^2 = -0.88m_\mu^2)$  is 1.5 times the value expected from PCAC. To assess the reliability of the theoretical framework used by the TRIUMF group to relate  $\Gamma_{\text{RMC}}$  to the pseudoscalar form factor  $f_P$ , we calculate  $\Gamma_{\text{RMC}}$  in chiral perturbation theory, which provides a systematic framework to describe all the vertices involved in RMC, fulfilling gauge-invariance and chiral-symmetry requirements in a transparent manner. As a first step we present a chiral perturbation calculation at tree level which includes sub-leading order terms.

*Key words:*  $\mu^- + p \rightarrow \nu n \gamma$ , heavy baryon chiral perturbation theory, pseudoscalar coupling

*PACS:* 23.40.-s, 12.39.Fe, 13.60.-r

---

## 1 Introduction

It has long been a great experimental challenge to observe radiative muon capture (RMC) on the proton,  $\mu^- + p \rightarrow n + \nu_\mu + \gamma$ , because of its extremely

---

<sup>1</sup> email: meissner@yukawa.phys.cmu.edu

<sup>2</sup> email: myhrer@nuc003.psc.sc.edu

<sup>3</sup> email: kubodera@nuc003.psc.sc.edu

small branching ratio. Recently, an experimental group at TRIUMF [1] finally succeeded in measuring  $\Gamma_{\text{RMC}}$ , the capture rate for RMC on a proton.<sup>4</sup> A main goal of measuring  $\Gamma_{\text{RMC}}$  is to extract information about the pseudoscalar form factor,  $f_P$ , of the weak hadronic matrix element. The matrix element of the hadronic charged weak current  $h^\lambda = V^\lambda - A^\lambda$  between a proton and a neutron is given by

$$\langle n(p_f) | V^\lambda - A^\lambda | p(p_i) \rangle = \bar{u}(p_f) \left[ f_V(q^2) \gamma^\lambda + \frac{f_M(q^2)}{2m_N} \sigma^{\lambda\mu} q_\mu + f_A(q^2) \gamma^\lambda \gamma_5 + \frac{f_P(q^2)}{m_\pi} q^\lambda \gamma_5 \right] u(p_i), \quad (1)$$

where  $q \equiv p_i - p_f$ , and the absence of the second-class current is assumed. Of the four form factors appearing in eq.(1),  $f_P$  is experimentally the least well known. Although ordinary muon capture (OMC) on a proton,  $\mu^- + p \rightarrow n + \nu_\mu$ , can in principle give information on  $f_P$ , its sensitivity to  $f_P$  is intrinsically suppressed. This is because the momentum transfer involved in OMC,  $q^2 = -0.88m_\mu^2$ , is far away from the pion-pole position  $q^2 = m_\pi^2$ , where the contribution of  $f_P(q^2)$  becomes most important. RMC on a proton provides a more sensitive probe of  $f_P$  than OMC, because the three-body final state in RMC allows one to come closer to the pion pole.

To relate  $\Gamma_{\text{RMC}}$  to  $f_P$ , the authors of [1] used the theoretical framework of Beder and Fearing [2]. In this framework, as in many earlier works [3–6], one invokes a minimal substitution to generate the RMC transition amplitude from the transition amplitude for OMC, the hadronic part of which is given by Eq. (1). The actual procedure used in [2] is as follows. First, the pion-pole factor is explicitly extracted from  $f_P$  as  $f_P(q^2) = \tilde{f}_P/(q^2 - m_\pi^2)$ , where  $\tilde{f}_P$  is a constant. Then one replaces every  $q$  in Eq.(1) with  $q - ie\mathcal{A}$  ( $\mathcal{A}$  is the electromagnetic field) except the  $q$  appearing in the  $q^2$  dependence of  $f_V$ ,  $f_A$  and  $f_M$ .  $\Gamma_{\text{RMC}}^{\text{theor}}$  resulting from this treatment has a parametric dependence on  $\tilde{f}_P$ . In the analysis in ref. [1],  $\tilde{f}_P$  is adjusted to optimize agreement between  $\Gamma_{\text{RMC}}^{\text{theor}}$  and the measured rate  $\Gamma_{\text{RMC}}^{\text{exp}}$  (more precisely  $R(> 60 \text{ MeV})$ ). The result of this optimization, expressed in terms of  $g_P \equiv f_P(q^2 = -0.88m_\mu^2) = \tilde{f}_P/(-0.88m_\mu^2 - m_\pi^2)$ , is  $g_P = (10.0 \pm 0.9 \pm 0.3)g_A$ , where  $g_A = f_A(0)$ . This value is  $\sim 1.5$  times the value expected from PCAC. This surprising result should be contrasted with the fact that  $g_P$  measured in OMC is consistent with the PCAC prediction within large experimental uncertainties [7].

A natural question one could ask is: How reliable is  $\Gamma_{\text{RMC}}^{\text{theor}}$  used in deducing  $g_P$  from  $\Gamma_{\text{RMC}}^{\text{exp}}$ ? It seems important to reexamine the reliability of the existing phenomenological approach [2] which uses a selective minimal substitution. Chiral perturbation theory (ChPT) provides a systematic framework

---

<sup>4</sup> To be more precise, the TRIUMF experiment determined the partial capture rate  $R(> 60\text{MeV})$ , corresponding to emission of a photon with  $E_\gamma > 60\text{MeV}$ .

to describe the electromagnetic-, weak-, and strong-interaction vertices in a consistent manner, thereby allowing us to avoid applying a phenomenological minimal-coupling substitution at the level of the transition amplitude. Furthermore, ChPT enables us to satisfy the gauge-invariance and chiral-symmetry requirements in a transparent way.

Starting with the seminal work of Gasser and Leutwyler [8] ChPT has proven to be a very powerful and successful technique for hadronic phenomenology at low energies. Its application includes the physics of the pseudoscalar mesons ( $\pi, K, \eta$ ) [9], pion-nucleon systems [10] and few-nucleon systems [11,12]. Muon capture is another favorable case for applying ChPT since momentum transfers involved here do not exceed  $m_\mu$ , and  $m_\mu$  is small compared to the chiral scale  $\Lambda \sim 1$  GeV, indicating the possibility of a reasonably rapid convergence of the chiral expansion. In the case of OMC, Bernard et al.[14] and Fearing et al.[15] used heavy-baryon ChPT to evaluate  $f_P$  with better accuracy than achieved in the PCAC approach. In the case of RMC, a ChPT calculation provides a natural extension of the classic work of Adler and Dothan[13] based on the low-energy theorems. These observations motivate us to attempt a systematic ChPT calculation of  $\Gamma_{\text{RMC}}$ . As a first step we calculate the total capture rate  $\Gamma_{\text{RMC}}$  and the spectrum of the emitted photons,  $d\Gamma_{\text{RMC}}(k)/dk$ , to sub-leading order in chiral perturbation expansion. Thus, our calculation includes nucleon recoil contributions of  $\mathcal{O}(1/M)$ . We limit ourselves here to the case of RMC from the  $\mu$ - $p$  atom with statistical spin distributions, leaving out the hyperfine-state decomposition and the treatment of RMC from the  $p\mu p$  molecule.

## 2 Calculational Method

We employ heavy-baryon chiral perturbation theory [16] and use the effective Lagrangian  $\mathcal{L}_{\text{ch}}$  as given in [10].  $\mathcal{L}_{\text{ch}}$  is written in the most general form involving pions and heavy nucleons in external weak- and electromagnetic-fields consistent with chiral symmetry. We expand  $\mathcal{L}_{\text{ch}}$  in increasing chiral order as:

$$\mathcal{L}_{\text{ch}} = \mathcal{L}_\pi^{(0)} + \mathcal{L}_{\pi N}^{(0)} + \mathcal{L}_{\pi N}^{(1)} + \dots . \quad (2)$$

Here  $\mathcal{L}^{(\bar{\nu})}$  represents terms of chiral order  $\bar{\nu}$  given by  $\bar{\nu} \equiv d + \frac{1}{2}n - 2$ , where  $d$  is the summed power of the derivative and the pion mass, and  $n$  denotes the number of nucleon fields involved in a given term [17]. We limit ourselves here to a next-to-leading chiral order (NLO) calculation and therefore we only consider the terms with  $\bar{\nu} = 0$  and  $\bar{\nu} = 1$ . To this chiral order we need only consider tree diagrams, and then  $\mathcal{L}_{\pi N}^{(1)}$  only represents  $1/M$  “nucleon recoil” corrections to the leading “static” part  $\mathcal{L}_{\pi N}^{(0)}$ . We give below the explicit expressions for the  $\mathcal{L}_\pi^{(0)}$ ,  $\mathcal{L}_{\pi N}^{(0)}$  and  $\mathcal{L}_{\pi N}^{(1)}$ , in which only terms of direct relevance

for our NLO calculation are retained.

$$\mathcal{L}_\pi^{(0)} = \frac{f_\pi^2}{4} \text{Tr} [D_\mu U D^\mu U] + \dots \quad (3)$$

$$\mathcal{L}_{\pi N}^{(0)} = \bar{N} \{iv \cdot D + g_A S \cdot u\} N \quad (4)$$

$$\begin{aligned} \mathcal{L}_{\pi N}^{(1)} = \bar{N} \Big\{ & \frac{1}{2M} (v \cdot D)^2 - \frac{1}{2M} D \cdot D - \frac{ig_A}{2M} \{S \cdot D, v \cdot u\}_+ \\ & - \frac{i}{4M} [S^\mu, S^\nu]_- \left( (1 + \kappa_v) f_{\mu\nu}^+ + \frac{1}{2} (\kappa_s - \kappa_v) \text{Tr} f_{\mu\nu}^+ \right) \Big\} N + \dots . \end{aligned} \quad (5)$$

Here  $U = \sqrt{1 - \vec{\pi}^2/f_\pi^2} + i\vec{\tau} \cdot \vec{\pi}/f_\pi$  denotes the chiral field in the sigma gauge, and  $N$  the heavy nucleon spinor of mass  $M$ . We have also used other standard notations, see [10]:

$$\begin{aligned} D_\mu U &\equiv \partial_\mu U - i(\mathcal{V}_\mu + \mathcal{A}_\mu)U + iU(\mathcal{V}_\mu - \mathcal{A}_\mu) \\ U &\equiv u^2; \quad u_\mu \equiv iu^\dagger D_\mu U u^\dagger \\ D_\mu N &\equiv \partial_\mu N + \frac{1}{2}[u^\dagger, \partial_\mu u]_- N - \frac{i}{2}u^\dagger(\mathcal{V}_\mu + \mathcal{A}_\mu)u - \frac{i}{2}u(\mathcal{V}_\mu - \mathcal{A}_\mu)u^\dagger \\ F_\mu^R &\equiv \mathcal{V}_\mu + \mathcal{A}_\mu; \quad F_\mu^L \equiv \mathcal{V}_\mu - \mathcal{A}_\mu \\ F_{\mu\nu}^{L,R} &\equiv \partial_\mu F_\nu^{L,R} - \partial_\nu F_\mu^{L,R} - i[F_\mu^{L,R}, F_\nu^{L,R}]_- \\ f_{\mu\nu}^+ &\equiv u^\dagger F_{\mu\nu}^R u + u F_{\mu\nu}^L u^\dagger . \end{aligned} \quad (6)$$

The covariant derivatives above include the external vector and axial vector fields,  $\mathcal{V}_\mu = \mathcal{V}_\mu^a \frac{\tau^a}{2}$  and  $\mathcal{A}_\mu = \mathcal{A}_\mu^a \frac{\tau^a}{2}$ , respectively. We choose the four-velocity  $v_\mu$  to be  $v^\mu = (1, \vec{0})$ . With this choice the spin operator  $S^\mu$  of the heavy nucleon becomes  $S^\mu = (0, \frac{1}{2}\vec{\sigma})$ . The only parameters appearing in the above expressions are the pion decay constant,  $f_\pi = 93$  MeV, the axial vector coupling,  $g_A = 1.26$ , and the nucleon isoscalar and isovector anomalous magnetic moments,  $\kappa_s = -0.12$  and  $\kappa_v = 3.71$ . Thus, to the chiral order of our interest,  $\mathcal{L}_{\text{ch}}$  is well determined.

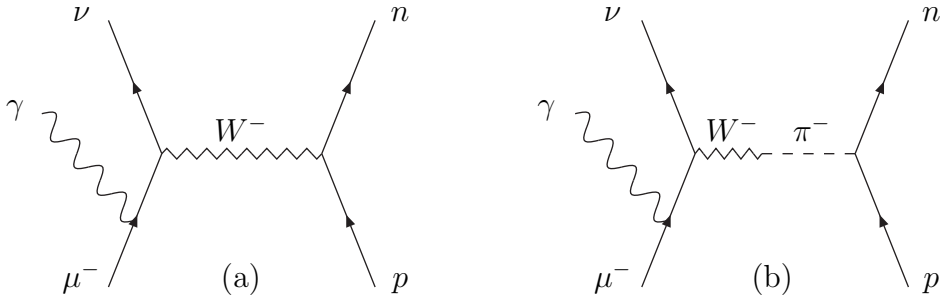


Fig. 1.

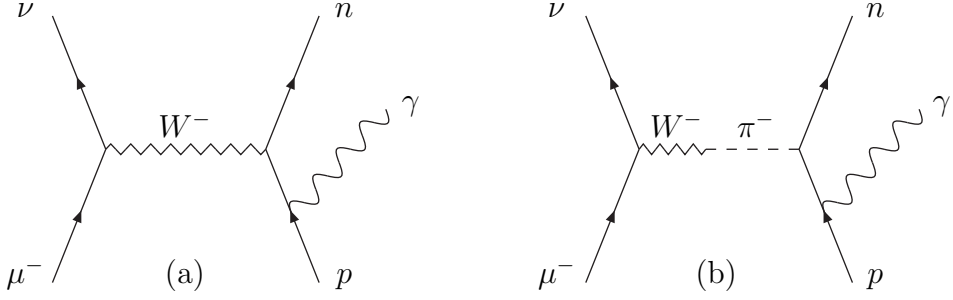


Fig. 2.

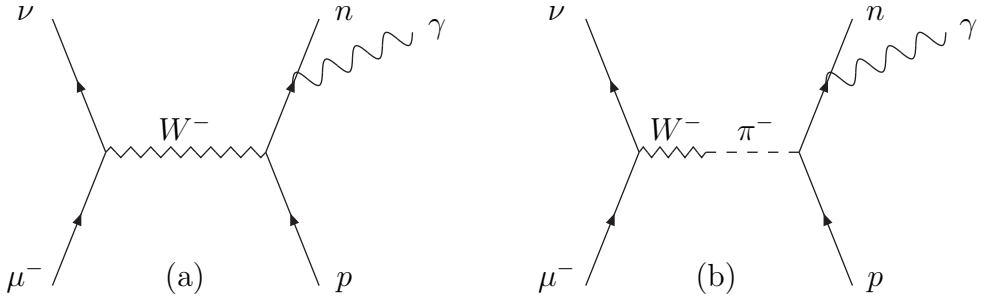


Fig. 3.

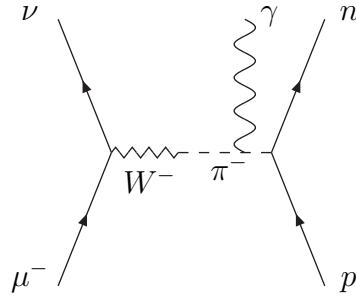


Fig. 4.

We consider all possible Feynman diagrams up to chiral order  $\nu = 1$  which contribute to the process  $\mu^- + p \rightarrow n + \nu + \gamma$ . These are displayed in Figs.1-6. The zigzag lines in these diagrams represent the  $W^-$  boson that couples to the leptonic and hadronic currents in the standard manner. In the actual calculation, taking the limit  $m_W \rightarrow \infty$ , we make the substitution

$$W_\mu^- \rightarrow (\mathcal{V}_\mu^- - \mathcal{A}_\mu^-) \frac{\tau^1 - i\tau^2}{2} \quad (7)$$

and treat  $\mathcal{V}$  and  $\mathcal{A}$  in the ChPT formalism as static external vector and axial sources, respectively. Then the diagrams in Figs.1-6 reduce to those that

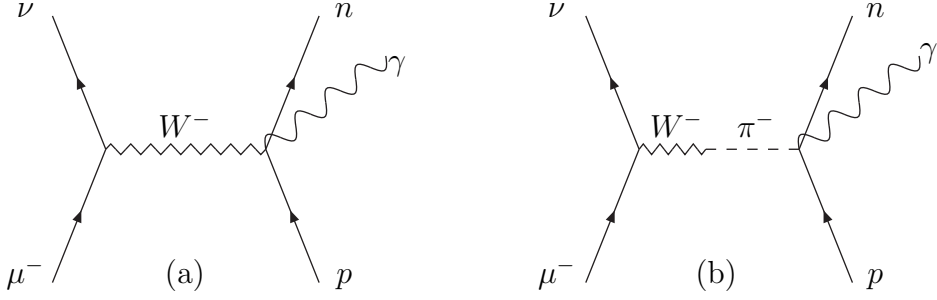


Fig. 5.

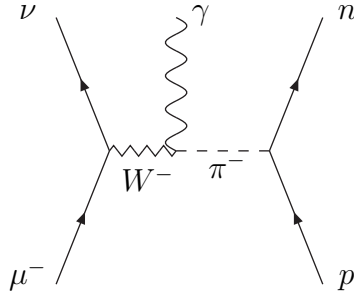


Fig. 6.

would result from the simple current-current interaction of the  $V - A$  form. The reason for explicitly retaining the  $W^-$  boson lines is to clearly separate the different photon vertices (see e.g. Fig.6). The leptonic vertices in these Feynman diagrams are of course well known. The hadronic vertices are obtained by expanding the ChPT Lagrangian [Eqs. (2), (3), (4) and (5)] in terms of the elementary fields  $N$ ,  $\pi$ ,  $\mathcal{V}$  and  $\mathcal{A}$  and their derivatives. The leading order terms arise from  $\mathcal{L}_{\pi N}^{(0)}$ , whereas the NLO contributions are  $1/M$  “recoil” corrections due to  $\mathcal{L}_{\pi N}^{(1)}$ . The evaluation of the transition amplitudes corresponding to these Feynman diagrams is straightforward. We denote by  $M_i$  ( $i = 1 \dots 6$ ) the invariant transition amplitudes corresponding to Fig.(1)-(6), respectively. They are given by:

$$M_1 = \epsilon^\beta(\lambda) \left[ \bar{u}_\nu(s) \gamma_\tau (1 - \gamma_5) \frac{\not{\mu} - \not{k} + m_\mu}{2(k \cdot \mu)} \gamma_\beta u_\mu(s') \right] \left[ H_n^\dagger(\sigma) h_1^\tau H_p(\sigma') \right] \quad (8)$$

$$M_i = [\bar{u}_\nu(s) \gamma_\tau (1 - \gamma_5) u_\mu(s')] \left[ H_n^\dagger(\sigma) h_i^\tau(\lambda) H_p(\sigma') \right], \quad i = 2, 3, 4, 5, 6, \quad (9)$$

which include the following hadronic operators:

$$h_1^\tau = \left[ (v^\tau - 2g_A S^\tau) + 2g_A \frac{(q_L)^\tau}{(q_L)^2 - m_\pi^2} (S \cdot q_L) \right]$$

$$\begin{aligned}
& + \left\{ \frac{1}{2M} [(p+n)^\tau - v^\tau v \cdot (p+n)] - \frac{1}{M} (1 + \kappa_v) i \epsilon^{\mu\tau\nu\alpha} (q_L)_\mu v_\nu S_\alpha \right. \\
& \left. + \frac{g_A}{M} v^\tau S \cdot (p+n) - \frac{g_A}{M} S \cdot (p+n) \frac{(q_L)^\tau}{q_L^2 - m_\pi^2} (v \cdot q_L) \right\} \quad (10)
\end{aligned}$$

$$\begin{aligned}
h_2^\tau(\lambda) = & \frac{1}{2M} \frac{1}{E_p - \omega_k} \left[ (v^\tau - 2g_A S^\tau) + 2g_A \frac{(q_N)^\tau}{(q_N)^2 - m_\pi^2} (S \cdot q_N) \right] \\
& \cdot \left[ \epsilon(\lambda) \cdot (2p - k) + (2 + \kappa_s + \kappa_v) (-i) \epsilon_{\alpha\beta\gamma\rho} \epsilon^\alpha(\lambda) k^\beta v^\gamma S^\rho \right] \quad (11)
\end{aligned}$$

$$\begin{aligned}
h_3^\tau(\lambda) = & \frac{1}{2M} \frac{1}{E_n + \omega_k} \left[ (v^\tau - 2g_A S^\tau) + 2g_A \frac{(q_N)^\tau}{(q_N)^2 - m_\pi^2} (S \cdot q_N) \right] \\
& \cdot \left[ (\kappa_s - \kappa_v) (-i) \epsilon_{\alpha\beta\gamma\rho} \epsilon^\alpha(\lambda) k^\beta v^\gamma S^\rho \right] \quad (12)
\end{aligned}$$

$$\begin{aligned}
h_4^\tau(\lambda) = & (-) \frac{(q_N)^\tau (2q_L + k) \cdot \epsilon(\lambda)}{(q_N^2 - m_\pi^2)(q_L^2 - m_\pi^2)} \\
& \cdot \left[ 2g_A (S \cdot q_L) - \frac{g_A}{M} S \cdot (p+n) (q_L \cdot v) \right] \quad (13)
\end{aligned}$$

$$\begin{aligned}
h_5^\tau(\lambda) = & 2 g_A \frac{(q_N)^\tau}{(q_N)^2 - m_\pi^2} (S \cdot \epsilon(\lambda)) + \frac{g_A}{M} \frac{(q_N)^\tau}{(q_N)^2 - m_\pi^2} (v \cdot q_N) (S \cdot \epsilon(\lambda)) \\
& - \frac{g_A}{M} (S \cdot \epsilon(\lambda)) v^\tau - \frac{\epsilon^\tau(\lambda)}{2M} + \frac{1}{2M} (1 + \kappa_v) i \epsilon^{\tau\alpha\beta\rho} \epsilon_\alpha(\lambda) v_\beta S_\rho \quad (14)
\end{aligned}$$

$$h_6^\tau(\lambda) = \frac{\epsilon^\tau(\lambda)}{q_L^2 - m_\pi^2} \left[ 2g_A (S \cdot q_L) - \frac{g_A}{M} S \cdot (p+n) (v \cdot q_L) \right]. \quad (15)$$

In these expressions,  $\mu, \nu, p = (E_p, \vec{p})$ ,  $n = (E_n, \vec{n})$  and  $k = (\omega_k, \vec{k})$  are the four-momenta of the muon, neutrino, proton, neutron and photon, respectively. The  $z$ -components of the spins of the muon, neutrino, proton and neutron are denoted by  $s, s', \sigma'$  and  $\sigma$ , respectively, while  $\epsilon(\lambda)$  stands for the photon polarization vector. We have also defined  $q_L = n - p$  and  $q_N = n - p + k$ .

The pion-pole diagrams, Figs.1(b), 2(b), 3(b), 4, 5(b) and 6, originate from  $\mathcal{L}_\pi^{(0)}$ , Eq.(3). The coupling of the axial component of eq.(7) to the  $\pi$  generates these Feynman diagrams. In ChPT the pion-pole contributions, which arise automatically from a well-defined chiral Lagrangian, are completely determined

by the chiral Lagrangian. The fact that they need not be put in by hand constitutes a major advantage of the ChPT approach over the phenomenological approaches which have been used in the earlier calculations [2–4]. In this context it is also worthwhile to mention that the pseudoscalar coupling  $g_P$  itself does not appear explicitly in ChPT calculations of the transition amplitudes since  $g_P$  is effectively accounted for via the pion-pole diagrams. As mentioned in the introduction,  $\mathcal{L}_{\text{ch}}$  determines  $g_P$  [14,15]. However, since the same  $\mathcal{L}_{\text{ch}}$  directly determines the transition amplitude of RMC,  $g_P$  does not feature in our expressions for  $M_i$ 's.

It is safe to assume both the muon and the proton to be at rest by neglecting the binding and kinetic energies of the  $\mu p$  atom. Thus,  $\mu = (m_\mu, \vec{0})$  and  $p = (M, \vec{0})$ . For the neutron four-momentum  $n$ , we retain its three-momentum  $\vec{n}$  but neglect the recoil energy, or  $E_n = M + \vec{n}^2/2M \approx M$ . The maximal value of  $|\vec{n}|$  equals  $m_\mu$  giving a recoil energy  $\vec{n}^2/2M \approx 6$  MeV, which is small even compared with  $m_\mu$ . With  $n \approx (M, \vec{n})$ , we have  $q_L = (0, \vec{n})$  and  $q_N = (\omega_k, \vec{n} + \vec{k})$ . Consequently, all terms proportional to  $v \cdot q_L$  vanish.

We choose to work in the Coulomb gauge with the result  $v \cdot \epsilon(\lambda) = 0$ . With this gauge choice and the above kinematical approximations, the hadronic radiation diagrams, Figs.(2) and (3), become  $\mathcal{O}(1/M^2)$  [see Eqs. (11) and (12)], and therefore do not contribute to the chiral order under consideration. Moreover, in the sum  $h_2 + h_3$ , the terms proportional to  $\kappa_v$  vanish in our approach (to the order under consideration), whereas in the treatment of, e.g., [3], these terms are numerically large.

### 3 Numerical Results

As stated, we consider here only the RMC from the  $\mu p$  atomic state with the hyperfine states unseparated. Within our kinematical approximations the spin-averaged total capture rate is given by

$$\begin{aligned} \Gamma_{\text{RMC}} = & \left( \frac{eG}{\sqrt{2}} \right)^2 |\Phi(0)|^2 \frac{1}{4} (2\pi)^4 \int \frac{d^3 n}{(2\pi)^3} \int \frac{d^3 \nu}{(2\pi)^3} \int \frac{d^3 k}{(2\pi)^3} \frac{1}{2\omega_k} \\ & \times \delta^{(4)}(n + \nu + k - p - \mu) \sum_{\sigma\sigma' ss' \lambda} |M|^2 , \end{aligned} \quad (16)$$

where the sum is over all spin and polarization orientations, and

$$M = \sum_{i=1}^6 M_i , \quad (17)$$

with  $M_i$  given by Eqs. (8) and (9). The value of the  $\mu p$  atomic wavefunction at the origin is given by

$$|\Phi(0)|^2 = \frac{1}{\pi} m_\mu^3 \alpha^3 \left( \frac{M}{M + m_\mu} \right)^3. \quad (18)$$

In the kinematical approximation stated earlier,

$$\delta^{(4)}(n + \nu + k - p - \mu) \approx \delta(|\vec{k}| + |\vec{\nu}| - m_\mu) \delta^{(3)}(\vec{n} + \vec{\nu} + \vec{k}), \quad (19)$$

and the maximal  $\gamma$  energy is  $(\omega_k)_{\max} \approx m_\mu$ . Eq.(16) then simplifies as

$$\begin{aligned} \Gamma_{\text{RMC}} = & \left( 8\pi^2 \mathcal{C} \right) \int_0^{(\omega_k)_{\max} \approx m_\mu} d\omega_k \omega_k (m_\mu - \omega_k)^2 \\ & \times \int d\cos\theta \sum_{i,j=1,4,5,6} \sum_{\sigma\sigma' ss' \lambda} \left( M_i M_j^* \right)_{\substack{\vec{n} = -(\vec{\nu} + \vec{k}) \\ |\vec{\nu}| = m_\mu - \omega_k}}, \end{aligned} \quad (20)$$

where we have introduced the abbreviation

$$\mathcal{C} = \left( \frac{eG}{\sqrt{2}} \right)^2 |\Phi(0)|^2 \frac{1}{8} \left( \frac{1}{2\pi} \right)^5. \quad (21)$$

The evaluation of the spin sum is tedious but straightforward; the resulting lengthy expressions will be given elsewhere. Table 1 summarizes the numerical values for the total capture rate  $\Gamma_{\text{RMC}}$ . We show in the table the breakdown of  $\Gamma_{\text{RMC}}$  into the leading-order contribution  $\mathcal{O}((1/M)^0)$ , coming from  $\mathcal{L}_{\pi N}^{(0)}$ , and the next-to-leading-order contribution  $\mathcal{O}(1/M)$ , arising from  $\mathcal{L}_{\pi N}^{(1)}$ . We also show the value of  $\Gamma_{\text{RMC}}$  which would result if all the diagrams containing the pion-pole, Fig.1(b), 4, 5(b) and 6, are omitted. Our result for the total capture rate  $\Gamma_{\text{RMC}} = 0.075 s^{-1}$  is close to the value given in [4],  $\Gamma_{\text{RMC}} = 0.069 s^{-1}$ , and practically identical to  $\Gamma_{\text{RMC}} = 0.076 s^{-1}$  reported in [5]. Our  $\mathcal{O}(1/M)$  recoil corrections account for about 20% of the leading order  $\mathcal{O}((1/M)^0)$  contribution, which indicates a reasonable convergence of the chiral expansion. It should be noted that the size of the  $1/M$  corrections is noticeably larger in the approach of [5]. As one can see from Table 1, about 30% of the total value of  $\Gamma_{\text{RMC}}$  comes from the pion-pole exchange diagrams.

In Fig.7 we plot the spectrum of the emitted photons  $d\Gamma_{\text{RMC}}(\omega_k)/d\omega_k$ . In addition to the result of the full calculation, the figure includes the spectrum corresponding to the leading-order calculation, i.e., the  $\mathcal{O}((1/M)^0)$  contribution only. For the sake of comparison, we also show the result of [2,5] corresponding to the use of the Goldberger-Treiman value  $g_P = 6.6 g_A$ . Although,

Table 1  
Total RMC capture rate in  $s^{-1}$

	$\Gamma_{\text{RMC}}$	$\Gamma_{\text{RMC}} _{\text{without}\pi}$
$\mathcal{O}((1/M)^0)$	0.061	0.043
$\mathcal{O}(1/M)$	0.014	0.010
total	0.075	0.053

as discussed above, the total  $\Gamma_{\text{RMC}}$  of our calculation is practically identical to that of [5], the photon spectrum shows a rather noticeable difference between these two calculations.

#### 4 Discussion and Conclusions

A direct comparison of our calculation with the experimental data [1] is premature because we have not considered captures from the singlet and triplet hyperfine states separately, or capture from the  $p\mu p$  molecular state. This

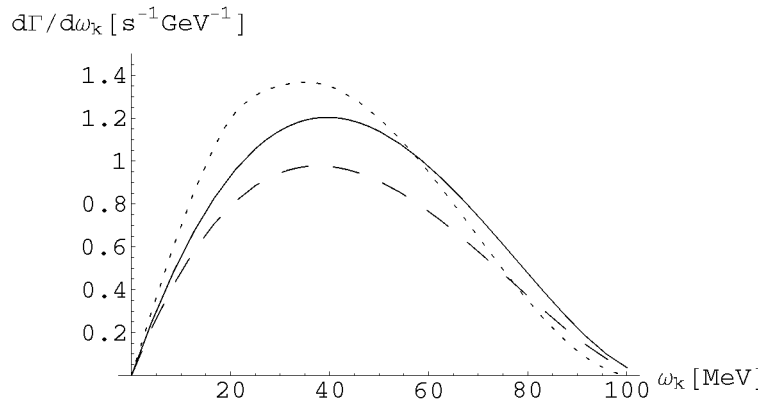


Fig. 7. Spectrum of the emitted photons. The full line represents the full calculation including  $\mathcal{O}((1/M)^0)$  and  $\mathcal{O}((1/M)^1)$ ; the dashed line represents the result that contains only the  $\mathcal{O}((1/M)^0)$  contributions; the dotted line shows the result of [2,5] with  $g_P = 6.6g_A$ .

also means that at this stage we cannot directly address the “ $g_P$  problem” that arose from the TRIUMF data [1]. However, it is probably worthwhile to make the following remark. The TRIUMF experiment detected only “energetic” photons,  $\omega_k > 60$  MeV. Meanwhile, Fig.7 indicates that, for the spin-averaged  $\mu p$ -atomic RMC, our ChPT calculation gives a photon spectrum that is rather significantly harder than that of [2]. This is particularly true in the region  $\omega_k > 60$  MeV; for example, at  $\omega_k = 80$  MeV our calculation gives  $d\Gamma_{\text{RMC}}(\omega_k)/d\omega_k = 0.48 \text{ s}^{-1} \text{ GeV}^{-1}$  to be compared with  $d\Gamma_{\text{RMC}}(\omega_k)/d\omega_k = 0.35 \text{ s}^{-1} \text{ GeV}^{-1}$  from [2] (with use of  $g_P = 6.6g_A$ ). Now, as we have already pointed out, ChPT gives a unique prediction on  $g_P$ , and the calculational results [14,15] are consistent with the Goldberger-Treiman value  $g_P = 6.6g_A$ . This means that the two curves in Fig. 7, the solid and dotted lines, correspond to the common value of  $g_P = 6.6g_A$ . Thus, even with the same value of  $g_P$ , a chiral perturbation approach gives a harder  $\gamma$  spectrum than the conventional method [2] at least for the spin-averaged capture.<sup>5</sup> The difference in the photon spectra in Fig. 7 may influence the accuracy with which one can deduce  $g_P$  from the experimental photon spectrum in the higher energy region. Of course, a more quantitative statement can be made only after a more detailed ChPT calculation becomes available in which the hyperfine states are separated and the  $p\mu p$ -molecular absorption is evaluated.

We must also emphasize that the present calculation includes only up to the next-to-leading chiral order (NLO) contributions. The next-to-next-to-leading order (NNLO) calculations are obviously desirable. For this one must include the  $\bar{\nu} = 2$  chiral Lagrangian,  $\mathcal{L}_\pi^{(2)}$  and  $\mathcal{L}_{\pi N}^{(2)}$ , and also loop corrections arising from  $\mathcal{L}_\pi^{(0)}$  and  $\mathcal{L}_{\pi N}^{(0)}$ . The finite contributions from the loop diagrams would give momentum-dependent vertices, which would correspond to the form factors in the language of the phenomenological approach [2,3,5]. These contributions are probably small but it would be reassuring to check that explicitly. One problem in extending the present calculation to the next order is that, although the forms of  $\mathcal{L}_\pi^{(2)}$  and  $\mathcal{L}_{\pi N}^{(2)}$  have been determined [8,18], some coefficients of the counter terms in  $\mathcal{L}_{\pi N}^{(2)}$  have not been evaluated. On the other hand, chiral expansion for muon capture is characterized by the expansion parameter  $m_\mu/M$ , and is expected to converge reasonably rapidly. Indeed, in the case of OMC, where the  $\nu = 2$  calculation is much less involved, explicit evaluations [14,15] show that the NNLO contributions amount only to a few percents. It is likely that, in the case of RMC as well, NNLO corrections modify our results only by a few percents.

In this connection we also note that the approach of Bernard et al.[10], which we are following here, does not contain the explicit  $\Delta$  degree of freedom in contrast to the approaches of [16]. Bernard et al.[10] consider that the  $\Delta$

---

<sup>5</sup> Within the formalism of [2], one needs to increase  $g_P$  to make the photon spectrum harder, see Fig.1 in the second reference in [2].

degree of freedom is effectively subsumed in the finite counter terms of the higher order chiral Lagrangian  $\mathcal{L}_{\pi N}^{(2)}$ . Therefore the  $\Delta$  degrees of freedom do not play a role in the chiral order we are considering, but the  $\Delta$  should be included in the next chiral order.

To summarize, the difference in the photon spectra shown in Fig.7 points to the necessity of further theoretical investigations in order to improve the accuracy with which one can deduce the value of  $g_P$  from the experimental  $\gamma$  spectrum [1]. We need an extended chiral perturbation calculation of RMC in which the hyperfine states are separated and the  $p\mu p$ -molecular absorption is evaluated, and in which the effects of higher chiral order terms are included.

## Acknowledgements

This work is supported in part by the National Science Foundation, Grants # PHY-9319641 and # PHYS- 9602000.

## References

- [1] G. Jonkmans et al., Phys. Rev. Lett. 77, (1996), 4512.
- [2] D.S. Beder and H.W. Fearing, Phys. Rev. D 35, (1987) 2130; Phys. Rev. D 39, (1989) 3493.
- [3] G.K. Manacher and L. Wolfenstein, Phys. Rev. 116, (1959) 782.
- [4] G.I. Opat, Phys. Rev. 134, (1964) B428.
- [5] H.W. Fearing, Phys. Rev. C 21 (1980), 1951.
- [6] H.P.C. Rood and H.A. Tolhoek, Nucl. Phys. 70, (1965) 658; R.S. Sloboda and H.W. Fearing, Nucl. Phys. A 340, (1980) 342; H.W. Fearing and M.S. Welsh, Phys. Rev. C 46, (1992) 2077.
- [7] T.P. Gorringe et al., Phys. Rev. Lett. 72, (1994) 3472;  
see also Proceedings of the 14th International Conference on Particles and Nuclei, ed. by C. Carlson and J. Domingo, World Scientific (1997).
- [8] J. Gasser and H. Leutwyler, Ann. Phys. N.Y. 158, (1984) 142; Nucl. Phys. B 250, (1985) 465.
- [9] For a review, see e.g. G. Ecker, Prog. Part. Nucl. Phys. 35, (1995) 1.
- [10] For a review, see e.g. V. Bernard, N. Kaiser and U.-G. Meissner, Int. J. Mod. Phys. E4, (1995) 193.

- [11] C. Ordonez, L. Ray and U. van Kolck, Phys. Rev. Lett. 72, (1994) 1982; Phys. Rev. C 53, (1996) 2086.
- [12] T.S. Park, D.-P. Min and M. Rho, Phys. Rep. 233, (1993) 341.
- [13] S.L. Adler and Y. Dothan, Phys. Rev. 151, (1966) 1267; see also F. Christillin and S. Servadio, Nuovo Cimento 42, (1977) 165.
- [14] V. Bernard, N. Kaiser and U.-G. Meissner, Phys. Rev. D 50, (1994) 6899.
- [15] H.W. Fearing, R. Lewis, N. Mobed and S. Scherer, hep-ph/9702394.
- [16] E. Jenkins and A.V. Manohar, Phys. Lett. B 255, (1991) 558; Phys. Lett. B 259, (1991) 353; T. Hemmert, B. Holstein and J. Kambor, Phys. Lett. B 395, (1997) 89.
- [17] S. Weinberg, Phys. Lett. B 251, (1990) 288; Nucl. Phys. B 363, (1991) 3; Phys. Lett. B 295, (1992) 114.
- [18] G. Ecker and M. Mojžiš, Phys. Lett. B 365, (1996) 312.